Ceramics-Silikáty 64 (3), 239-248 (2020)
www.ceramics-silikaty.cz doi: 10.13168/cs.2020.0013

THE HYDROTHERMAL SYNTHESIS OF 1.13 nm TOBERMORITE FROM GRANITE SAWING POWDER WASTE

#G. SMALAKYS, R. SIAUCIUNAS

Department of Silicate Technology, Kaunas University of Technology, Radvilenu pl. 19, LT- 50299 Kaunas, Lithuania

#E-mail: giedrius.smalakys@ktu.lt

Submitted October 18, 2019; accepted December 21, 2019

Keywords: Hydrothermal synthesis, 1.13 nm tobermorite, X-ray diffraction analysis, Simultaneous thermal analysis

This study presents the peculiarities that occur during the hydrothermal synthesis of 1.13 nm tobermorite from granite sawing powder waste and CaO. The molar ratios of the primary mixtures were CaO/SiO_2 = 0.83 and 1.0; a hydrothermal curing temperature of 180 and 200 °C; a duration of 4, 8, 12, 24, 72 h. The instrumental analyses (XRD, STA, SEM, TMA) data showed that this industrial by-product is a suitable material to synthesise of 1.13 nm tobermorite. Traces of the aforementioned mineral together with semi-amorphous C–S–H(I) were detected after 4 h at 180 °C. The crystallinity of the target mineral in the products grows steadily throughout the entire duration of the synthesis (up to 72 h at 180 °C). By increasing the temperature of the hydrothermal curing to 200 °C, the highest crystallinity of the 1.13 nm tobermorite was identified after 8 h of isothermal curing. Due to the chemical composition of the granite sawing powder waste, the 1.13 nm tobermorite remains stable and does not recrystallise into xonotlite even after 72 h at 200 °C in mixtures with CaO/SiO_2 = 1.0.

INTRODUCTION

The calcium silicate hydrate (CSH) family consists of approximately 40 different amorphous and crystalline, natural and synthetic minerals formed in the system of $CaO–SiO_2–H_2O$. The diversity of these compounds is determined by the molar ratio of CaO/SiO_2 which varies from 0.44 to 3.0 [1, 2]. Many of calcium silicate hydrates are important for cement science and technology because they form during hydration of OPC (Ordinary Portland cement) and hydrothermally in autoclaved dense and aerated products or hot-pressed materials [3]. Tobermorite is the most common representative mineral in the C–S–H family; it may be both natural and synthetic [4, 5]. Due to the low density, porosity and moderate refractoriness of the 1.13 tobermorite products, it is a favourable heat-insulating material [6, 7].

There are three main polymorphs of tobermorite which are classified according to their hydration degree: 1.4 nm tobermorite ($Ca_5Si_6O_{16}(OH)_2·7H_2O$) is the most hydrated member of the group [4]. The second member, 0.93 nm tobermorite ($Ca_5Si_6O_{16}(OH)_2$), does not have any crystallographic water in its structure [5] and is produced by heating other polymorphs of tobermorite in a certain thermal mode. The third polymorph, 1.13 nm tobermorite ($Ca_5Si_6O_{16}(OH)_2·4H_2O$), is one of the major phases found after the hydrothermal synthesis or in autoclaved concrete and during the evaporation of silica bricks [6-8].

The crystallisation of 1.13 nm tobermorite, as well as formation of the intermediate compounds, their stability intervals, purity, crystallinity, and crystal lattice parameters significantly depend on the hydrothermal synthesis conditions (temperature, duration, stirring intensity, water to solid (w/s) ratio, etc.). However, the chemical composition, purity, and dispersion of the raw materials have no less impact on the rate of formation, mineral composition and structure of the resulting products. The quality of the raw materials is particularly important when using natural rocks and industrial by-products as the external ions from the impurities very often determine the kinetics of the synthesis [9-11]. Numerous studies of the hydrothermal synthesis of 1.13 nm tobermorite have been carried out using different sources of SiO_2 and CaO. Quartz, amorphous SiO_2, and limestone are the best examples of these materials that have been thoroughly examined by H.F.W. Taylor, T. Mitsuda, J.D.C. McConnell and others [12-14]. These researchers have formulated the main conclusions about the hydrothermal synthesis using mixtures made from different raw materials. The field of study was further developed and additional data using new silica sources: silica fume Elkem, silica fume Grace Davison, silica sand Dorsilit [15], and marble [16] were published. Therefore, researchers have started to look for raw materials containing a more reactive part of the silica or containing additives, which accelerate the synthesis of 1.13 nm tobermorite. Some unconventional materials: kaolinite

and metakaolin [17], K-feldspar [18], the igneous rocks trachyte [19] and fuka [20], the sedimentary rock opoka [8, 21] were used for these goals. A great amount of data in the literature supports the idea that tobermorite family minerals can be synthesised from industrial by-products and wastes: coal fly ash [22], biomass ash [23], high alumina fly ash [24], blast furnace slag [25], steel slag [26], oil shale fly ash [27], and newsprint recycling waste [28].

The impurities present in the raw materials, for example, aluminium, sodium, potassium, and sulfate ions have a huge influence on the formation of tobermorite. According to the literature data, aluminium ions interrupt in the crystal structure of the 1.13 nm tobermorite and have a great influence on the CSH transformation to tobermorite [29]. N.Y. Mostafa et al. reported that aluminium impedes the crystallisation of tobermorite in the early stages of the synthesis [30]. Subsequently, the aluminium improves the conversion of the semi-crystalline C–S–H into a more structured and well-developed crystalline forms. Moreover, the literature indicates that aluminium additives inhibit the tobermorite conversion to xonotlite [31].

The alkaline additives accelerate the formation and further transformation of the crystalline forms of calcium silicate hydrates [29, 32, 33]. Sodium ions have an influence on the final mineral composition of the autoclaved products. If the molar ratio C/S = 0.83 is constant and only the $NaOH/SiO_2$ ratio varies (from 0.05 to 0.63), C-S-H(I), tobermorite, pectolite, and xonotlite form, respectively [34].

Some authors have attempted to synthesise 1.13 nm tobermorite at near room temperature [35]. It was determined that this method of synthesis is only suitable for scientific purposes unlike its application in production. The temperature increase has had a significant impact on the reaction kinetics; the synthesis durations have decreased from a hundred days to hours. Many researchers have started to focus on the temperature between 180 and 200 °C [36]. Nevertheless, the synthesis of tobermorite is a complex process where the temperature affects the stability of the compound. Depending on the impurities in the raw materials used, 1.13 nm tobermorite may lose stability at 200 °C [37] and start to recrystallise to xonotlite [38]. However, the published data imply that, under certain conditions, tobermorite can be synthesised at 200 °C or even at higher temperature [39]. The intensity of the characteristic to the 1.13 nm tobermorite peaks in the X-ray diffraction patterns has a tendency to augment when the synthesis temperature is increased. A higher temperature leads to the better conditions of this mineral synthesis, even though other calcium silicate hydrates were formed together. Summarising the research findings in the literature, the hydrothermal synthesis is usually carried out at 180 °C [40, 41]. Under these conditions, 1.13 nm tobermorite crystals form at an appropriate speed and reach a sufficient crystallinity degree.

The aim of this research is to adapt new natural rocks for cost-effective 1.13 nm tobermorite synthesis and to ensure the reuse of secondary raw materials. According to its mineral and chemical composition, one of the possible options is granite sawing powder waste. On the other hand, this type of waste contributes to environmental problems. In the production of granite products, about 25 % of the materials turn into dust, the main constituents of which are SiO_2, Al_2O_3, FeO and CaO, with minor impurities of Mg, Ti, Mn and K compounds [42]. This may cause environmental problems, for example, soil and water contamination unless efficiently bounded in unreactive compounds [43].

EXPERIMENTAL

Materials and methods

The granite sawing powder waste was taken from JSC Granitas (Lithuania), dried in an air chamber at 100 ± ± 1 °C for 24 h and milled in a ball mill ($S_a \approx 900\ m^2 \cdot kg^{-1}$). Loss on ignition – 4.31 %; oxide composition by X-ray fluorescence analysis (Bruker S8 Tiger WD spectrometer, Germany): SiO_2 – 58.4 %; Al_2O_3 – 15.4 %; Fe_2O_3 – – 7.17 %; CaO – 3.95 %; K_2O – 3.86 %; Na_2O – 3.56 %; MgO – 2.87 %; others – 0.48 %. The main component of the granite waste is SiO_2. The XRD analysis (Figure 1) shows one-crystal modifications of this oxide: quartz (PDF No. 00-005-0490). Moreover, after a deep chemical composition analysis was identified, the other minerals are listed in random order. Annite $KFe_3AlSi_3O_{10}(OH)_2$ (PDF No. 00-002-0045) – a phyllosilicate mineral from the mica family. Albite (PDF No. 00-009-0466) – a plagioclase feldspar mineral. Anorthite $CaAl_2Si_2O_8$ (PDF No. 04-015-4238) – the other mineral member of albite. Actinolite $K_{0.01}Na_{0.05}Ca_{1.9}Mg_{3.4}Mn_{0.1}Fe_{1.5}Al_{0.2}Si_{7.9}O_{22.1}(OH)_{1.9}$ (PDF No. 04-013-2277) – is an amphibole class

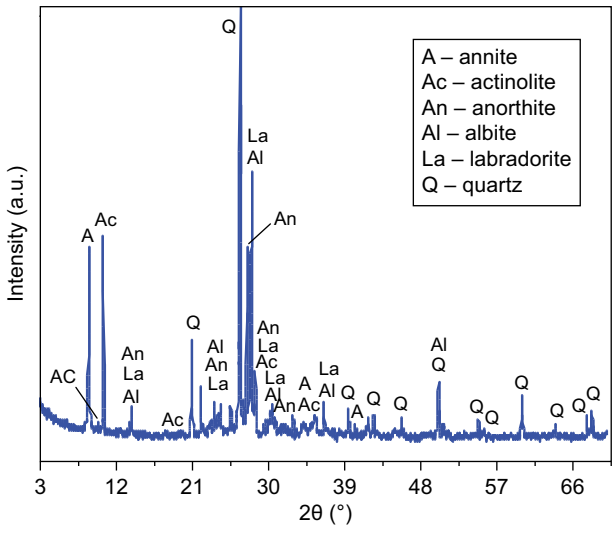

Figure 1. The XRD curves of the raw granite grinding waste.

mineral. Labradorite $Ca_{0.52}Na_{0.48}(Si,Al)_4O_8$ (PDF No. 05-001-0013) – is a feldspar mineral. Therefore, granite is a poly-mineral rock, which contains 15.4 % Al_2O_3 and a large amount of alkalis, which may accelerate the hydrothermal synthesis.

The granulometry of the milled granite sawing powders is $D_{90} < 17.41$ µm, $D_{50} < 3.99$ µm, and $D_{10} < 0.85$ µm. The average particle size is 10.33 µm (Figure 2).

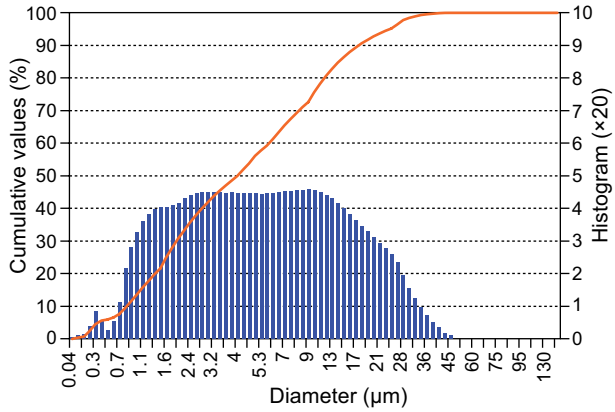

Figure 2. The particle size distribution of the granite sawing powders by the CILAS 1090 LD analyser.

CaO was obtained by calcination (1000 °C, 2 h; Nabertherm LV 15/11/P330, Germany) of $Ca(OH)_2$ (Stanchem, Poland, analytic grade) and milled until $S_a \approx 600$ $m^2 \cdot kg^{-1}$. The activity of the lime (CaO_{free} = = 93.09 %.) was determined by a standard procedure (ASTM C114–11b).

The homogenous raw materials (CaO/SiO_2 = 0.83 or 1.0) were diluted with water (W/S = 10.0) and put in 25 ml volume PTFE (polytetrafluoroethylene) cells, which were placed in a Parr Instruments (USA) autoclave. The parameters of the hydrothermal treatment: 180 or 200 °C for 2, 4, 8, 12, 24, and 72 h; without stirring. The synthesis products were prepared as follows: filtered and washed with acetone (to reduce the CO_2 uptake from the atmosphere); dried at 100 ± 1 °C for 24 h and sieved through an 80 µm mesh.

The products of the syntheses were characterised by powder X-ray diffraction (XRD; Bruker D8 Advance diffractometer, Germany), the simultaneous thermal analysis was performed in a nitrogen atmosphere, at a heating rate of 10 °C·min^{-1}; the temperature ranged from 40-940 °C (STA; Linseis PT1000 instrument, Germany), and scanning electron microscopy (SEM; JEOL JSM-7600F microscope, Japan).

The linear thermal expansion analysis of the powder samples was performed by Linseis 75PT 1600 dilatometer (Germany) using a corundum Al_2O_3 support tube (temperature interval 30 - 1100 °C, heating rate – 10 °C·min^{-1}, N_2 flux – 20 cm^3·min^{-1}).

The particle size distribution of the materials was measured using a laser particle size CILAS 1090 LD analyser with a sensitivity range from 0.04 to 500 lm, accuracy < 3 %, repeatability < 3 %. The detailed descriptions of hydrothermal synthesis and instrumental analysis procedures are available in ref [8].

RESULTS AND DISCUSSION

The XRD analysis showed that in the granite-lime mixture with the molar ratio of CaO/SiO_2 = 0.83 at 180 °C, 1.13 nm tobermorite (PDF No. 04-011-0271) was obtained after hydrothermal synthesis as the main compound. Nevertheless, during 4 h of synthesis, only traces of 1.13 nm tobermorite were identified in the product (Figure 3, curve 1) and the other minerals did not react except for labradorite. Furthermore, the low peak intensity of tobermorite and the rather intense peaks of quartz were determined, this implies that not all of the CaO content was involved in the formation of the calcium silicate hydrates where the rest of the calcium oxide was hydrated to produce portlandite, which was identified in the XRD curve (Figure 3, curve 1) [44]. This is also supported by the XRD analysis where calcite (PDF No. 00-002-0623) was identified and the thermal analysis showed a thermal effect of decarbonisation at 747 °C, due to the remaining carbonates from the

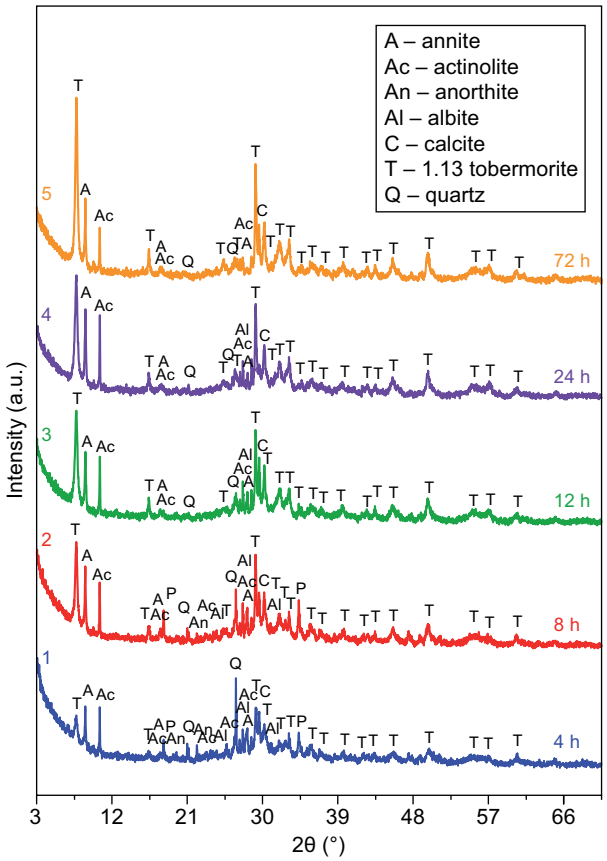

Figure 3. The XRD patterns of the synthesis products at 180 °C after 4 (1), 8 (2), 12 (3), 24 (4) and 72 h (5), when CaO/SiO_2 = 0.83.

raw materials and some quantity of portlandite was carbonated after the sample preparation. The intensity of the 1.13 nm tobermorite peaks after 8 h of isothermal curing significantly increased, but still, the quartz and other granite minerals peaks remained in the XRD pattern (Figure 3, curve 2). The 1.13 nm tobermorite peaks gradually increased while the intensity of the quartz peaks continuously decreased, prolonging the duration of the hydrothermal synthesis to 72 hours. (Figure 3, curves 3-5). Annite and actinolite were not involved in the synthesis as the intensity of their peaks during the synthesis practically remained unchanged (Table 1).

Table 1. The dependency of the intensity of the main diffraction peaks (a.u.) of annite, Actinolite and quartz on the synthesis duration at 180 °C.

	Duration of hydrothermal synthesis (h)				
	4	8	12	24	72
Annite	19.94	22.72	21.53	23.29	23.02
Actiniolite	19.74	19.92	20.57	22.61	18.29
Quartz	25.98	18.22	10.02	9.72	9.52

The results of the simultaneous thermal analysis confirmed the above statements: the endothermal effect at 40 - 200 °C temperature is associated with the dehydration of 1.13 nm tobermorite together with semi-crystalline C–S–H(I); however, it is very broad and vaguely expressed (Figure 4a). Other authors obtained similar results during the synthesis of 1.13 nm tobermorite from natural rocks and industrial waste materials with Al-containing impurities [45, 46]. According to the TGA (thermogravimetric analysis) data, the mass loss between 40 °C and 190 °C is 4.28 % and may be associated with the dehydration of the weakly bound molecular water from the crystal structure of 1.13 nm tobermorite and other C–S–H(I). The second endothermal peak at 747 °C corresponds to the decomposition of the carbonates in the products. The TGA data also indicate that the mass loss during the decarbonisation is 3.65 %. The exothermic effect of the recrystallisation of C–S–H(I) into wollastonite is double and consists of two peaks, the maximum at 872 and 902 °C. This means that the synthesised semi-amorphous calcium silicate hydrates, without a clear crystal structure consist of two phases: C–S–H(I) and C–S–H(II). The obtained results are well in line with the data in the literature, since the reduced molar ratio of C–S–H reduces their recrystallisation temperature [47, 48].

The STA data of 72 h hydrothermal synthesis product is shown in Figure 4b. The main dehydration effect at 40 - 219 °C is broader and the mass loss is greater (6.0 %) than in the case of the 4 h synthesis. Unfortunately, the removal of the absorbed and 1.13 nm tobermorite crystalline water overlaps in one effect. The tight thermal effect in the DSC curve at 717 °C indicates the existence of some amount of a carbonate in the product after 72 h of the synthesis. The weight loss at this temperature is about 1.25 %. This is explained by the fact that portlandite was not obtained in these conditions, which easily carbonates when preparing the samples for analysis and a high degree of crystallinity of 1.13 nm tobermorite is more resistant to CO_2 exposure. Moreover, the exothermic effect at 882 °C is clearly sharper and bigger in the DSC curve after the prolonged duration of the hydrothermal synthesis. This means, when increasing synthesis duration, more SiO_2 reacts and calcium silicate hydrates, with a stoichiometric composition close to the molar ratio of the starting mixtures (CaO/SiO_2 = 0.83), are formed.

The scanning electron microscopy (SEM) data of the 4 h synthesis sample (Figure 5a) shows that most of the new compounds are obtained as large agglomerates which are likely to be composed of semi-amorphous calcium silicate hydrates. The unreacted starting materials from the granite sawing waste raw material are also clearly visible in this image. Summarising the results from the SEM, XRD, and DSC analyses data after 4 h of isothermal curing at 180 °C, the 1.13 nm tobermorite crystallisation processes are in their initial stage.

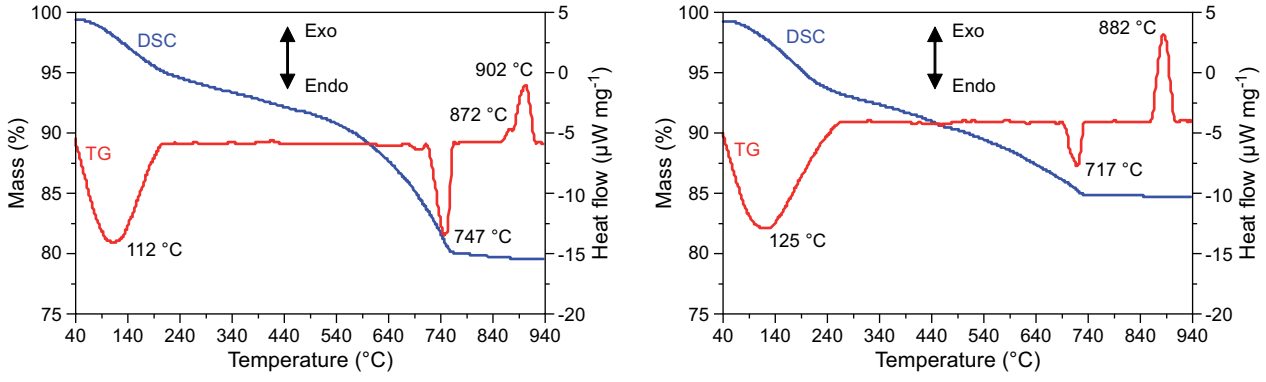

a) 4 h b) 72 h

Figure 4. The DSC and TG curves of the synthesis products at 180 °C after 4 h (a) and 72 h (b), when CaO/SiO_2 = 0.83

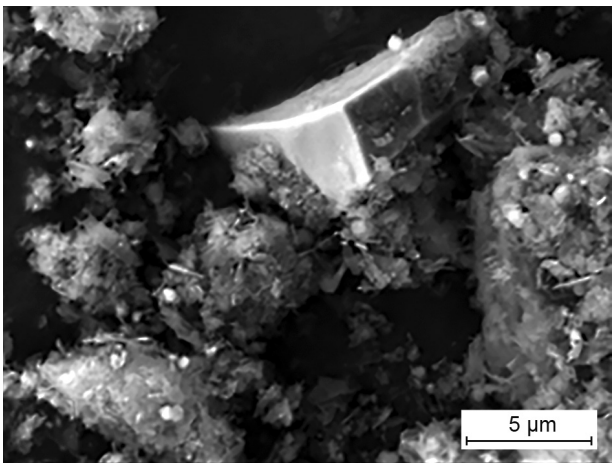

a) 4 h

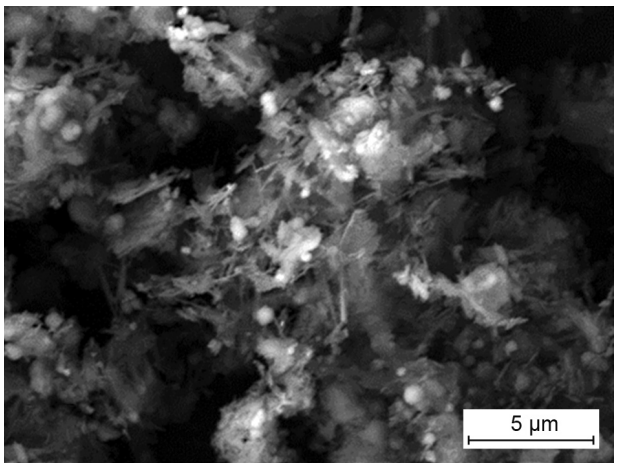

b) 72 h

Figure 5. The SEM images of the hydrothermal synthesis products at 180 °C after 4 h (a) and 72 h (b), when $CaO/SiO_2 = 0.83$.

After prolonging the synthesis duration up to 72 hours, the unreacted raw materials are not detected in the products and the amorphous agglomerates are significantly smaller (Figure 5b). The accumulation of two morphologies of 1.13 nm tobermorite crystals can be noticed in the SEM image: 1 - 2 μm length needle-shaped crystals and 2 - 4 μm size plates. These data are very similar to the results presented by other authors [15, 19], who have noticed that 1.13 nm tobermorite crystals can be of two types: in the shape of needles and plates. This may lead to a conclusion that, after 72 h of hydrothermal synthesis at 180 °C, a high crystallinity 1.13 nm tobermorite is formed and its crystals are distributed over the entire volume of the product.

It was determined that the semi amorphous compounds C–S–H(I) and C–S–H(II) were found at a short synthesis duration. These compounds consume most of the Ca^{2+} ions in the reaction medium and the required mixture stoichiometry for the synthesis of 1.13 nm tobermorite may be decreased. For this reason, a new mixture with a raised molar ratio up to $CaO/SiO_2 = 1.0$ was prepared in order to increase the formation of the tobermorite rate at 180 °C.

The XRD analysis data shows that, when the CaO content was increased, the intensity of the main peaks of 1.13 nm tobermorite after 4 h of synthesis are low (Figure 6, curve 1) and large amounts of unreacted minerals remain in the product. After prolonging the hydrothermal curing duration, the 1.13 nm tobermorite peak intensity increases (Figure 6, curves 2–5) but, in all the cases, it is significantly lower compared to the intensity using mixtures with a lower molar ratio ($CaO/SiO_2 = 0.83$). Due to a slower reaction, 1.13 nm tobermorite was identified as the main compound in the product only after 72 h of the synthesis (Figure 6, curve 5). It can be assumed that tobermorite was obtained at a lower degree of crystallinity together along with the semi amorphous C-S-H and are carbonised during the samples' preparation for analysis. Moreover, the XRD analysis showed much more intensive calcite peaks in these products (Figure 6). The TG analysis showed (Figure 7) that, when $CaCO_3$ decomposes, the mass losses are 5.11 % (4 h synthesis) and 2.12 % (72 h synthesis). A much larger number of carbonates was obtained than from the mixture with a molar ratio of $CaO/SiO_2 = 0.83$. Another difference that was noticed after 4 h of synthesis,

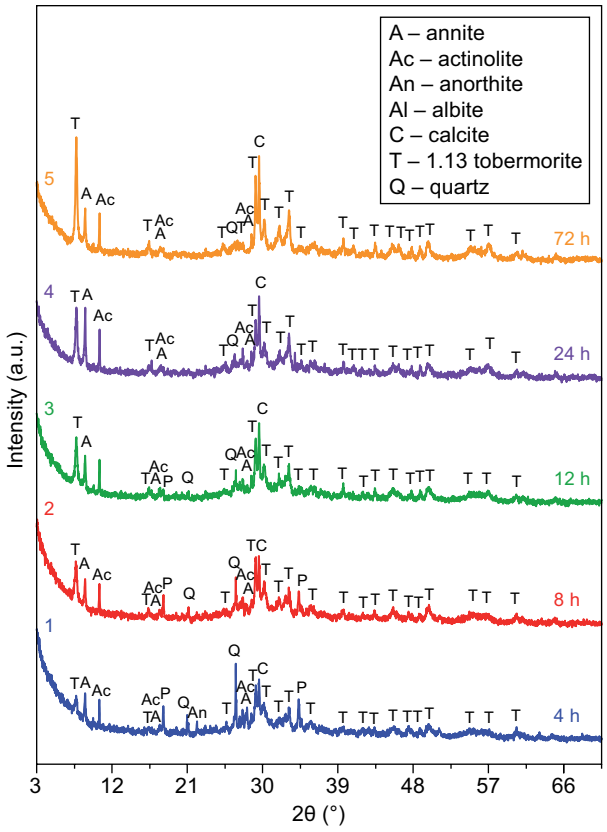

Figure 6. The XRD patterns of the synthesis products at 180 °C after 4 (1), 8 (2), 12 (3), 24 and 72 h (5), when $CaO/SiO_2 = 1.0$.

only calcium silicate hydrate of the C-S-H(II) type was formed (Figure 7a, curve 1), while in the product with $CaO/SiO_2 = 0.83$, this compound was detected together with C-S-H(I). Moreover, the 1.13 nm tobermorite remained stable and did not transform to xonotlite with the increased molar ratio up to $CaO/SiO_2 = 1.0$.

The obtained dilatometry analysis data from the powders after 4 - 72 h of synthesis (Figure 8) confirms and supplements the previously collected data from the XRD and STA analysis. Moreover, the literature indicates [47] that the semi-amorphous C–S–H type of the calcium silicate hydrates do not have a clear crystalline structure and shrink when they recrystallise into wollastonite. It means that the more crystalline structures (in this case tobermorite) have been obtained during hydrothermal synthesis in the products, the fewer changes in the volume will occur. Therefore, prolonging the synthesis duration from 4 h up to 72 h, the shrinkage of the sample decreases by nearly 7.07 % (Figure 8).

In order to establish a difference in the mineral composition of the powders synthesised at the different durations, the samples, after combustion at 940 °C for 0.5 h, were examined by XRD analysis (Figure 9). It was determined that, regardless of their molar ratio ($CaO/SiO_2 = 0.83$ or 1.0) and the duration of isothermal curing (4 or 72 h), the qualitative composition of products is the same: wollastonite (PDF No. 00-066-0271), gehlenite (PDF No. 04-014-4683), larnite (PDF No. 00-049-1673), annite and actinolite are formed. Nonetheless, the peak intensity of these compounds is highly dependent on the duration of the hydrothermal synthesis. The peaks of wollastonite, after calcination of the synthesis product with $CaO/SiO_2 = 0.83$ for 72 h are significantly intensive, meanwhile the peaks of gehlenite much lower (Figure 9, curve 2) in comparison with the 4 h synthesis product (Figure 9, curve 1). In our opinion, with the prolongation of the hydrothermal treatment, the Al-bearing compounds decompose and the Al^{3+} ions interrupt the crystal lattice of the calcium silicate hydrates. The more of these compounds that are in the synthesis product, the more wollastonite is formed during the combustion. The sample from the $CaO/SiO_2 = 1.0$ mixture in comparison with 0.83 one after 72 h hydrothermal curing reveal the significantly lower intensity of the wollastonite peaks (Figure 9, curve 4). This is due to the lower amount of the 1.13 nm tobermorite and C–S–H(I) formed (Figures 3 and 6, curves 5). This is also confirmed by the dilatometric analysis curves: the product with

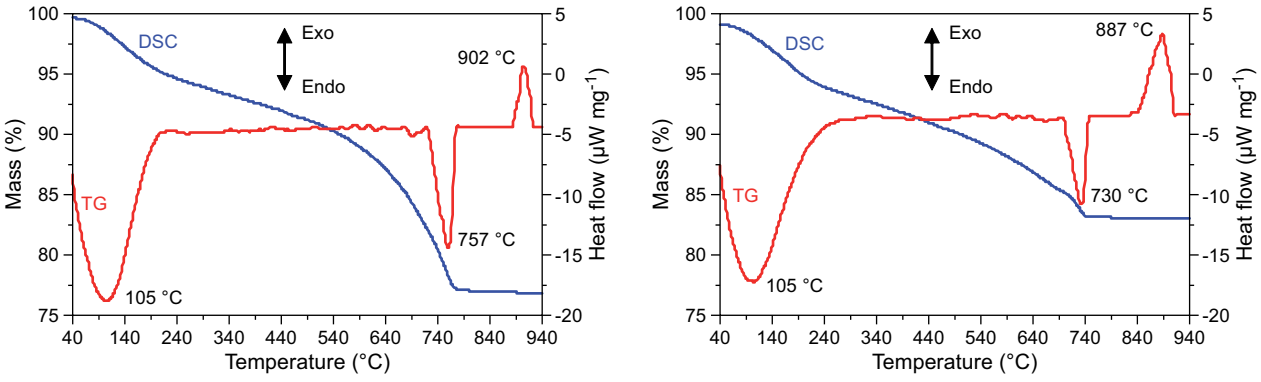

a) 4 h b) 72 h

Figure 7. The DSC and TG curves of the synthesis products at 180 °C after 4 h (a) and 72 h (b), when $CaO/SiO_2 = 1.0$.

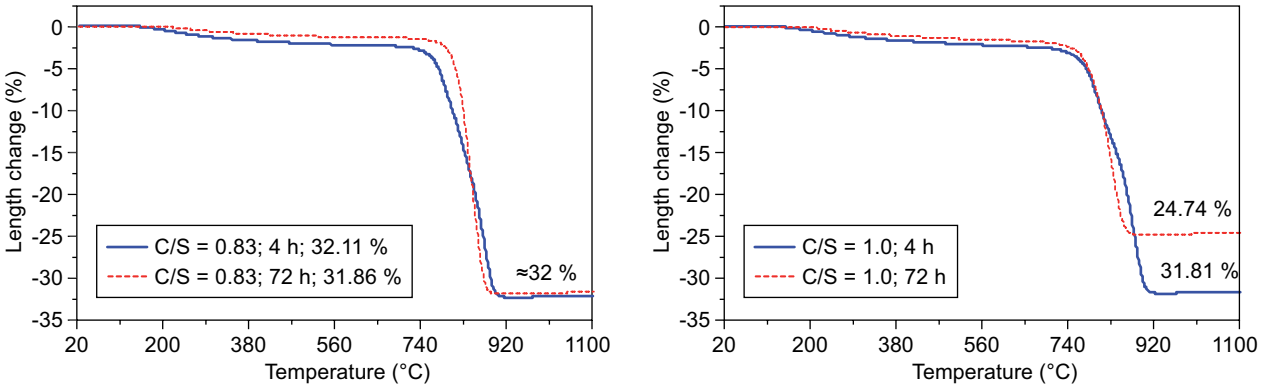

a) $CaO/SiO_2 = 0.83$ b) $CaO/SiO_2 = 1.0$

Figure 8. The dilatometric curves of the synthesis products at 180 °C, when $CaO/SiO_2 = 0.83$ (a) and 1.0 (b).

CaO/SiO_2 = 1.0 has less shrinkage, indicating that it contains less C–S–H(I). (Figure 8b). By increasing the synthesis duration, the amount of gehlenite is practically unchanged in the mixtures with CaO/SiO_2 = 1.0. The highest intensity of larnite peaks was identified after combustion of the sample obtained from a mixture with CaO/SiO_2 = 1.0 within 4 h. This is due to the higher molar ratio of the initial mixture and the higher amount of C–S–H(II) formed. The annite and actinolite from the granite sawing powder waste remained after calcination, but only traces of these minerals were identified.

Summarising the collected data, it can be stated that the composition of the CaO and granite sawing powder waste mixture for the production of 1.13 nm tobermorite should be CaO/SiO_2 = 0.83. In general, many hydrothermal reactions accelerate with the increasing temperature of the saturated water vapour. Since the synthesis of 1.13 nm tobermorite at the temperature of 180 °C was slow enough, it was decided to investigate its synthesis at 200 °C. It was determined that 1.13 nm tobermorite forms within the first 4 h of the hydrothermal curing from a mixture of CaO/SiO_2 = 0.83 (Figure 10, curve 1). However, based on the intensity of these compound peaks, its content seems to be low. In addition, there are intensive peaks of quartz and other raw materials in the XRD curve, these minerals are just starting to react. Thus, a temperature increase from 180 °C to 200 °C does not significantly affect the formation of new compounds at the beginning of the synthesis. A noticeable difference is that, in contrast to 180 °C, more C–S–H(I) and no C–S–H(II) semi-amorphous calcium silicate hydrates are formed (Figure 11). However, the situation changes significantly when prolonging the isothermal curing duration to 8 h. The intensity of the 1.13 nm tobermorite peaks obtained at 200 °C (Figure 10, curve 2) is much

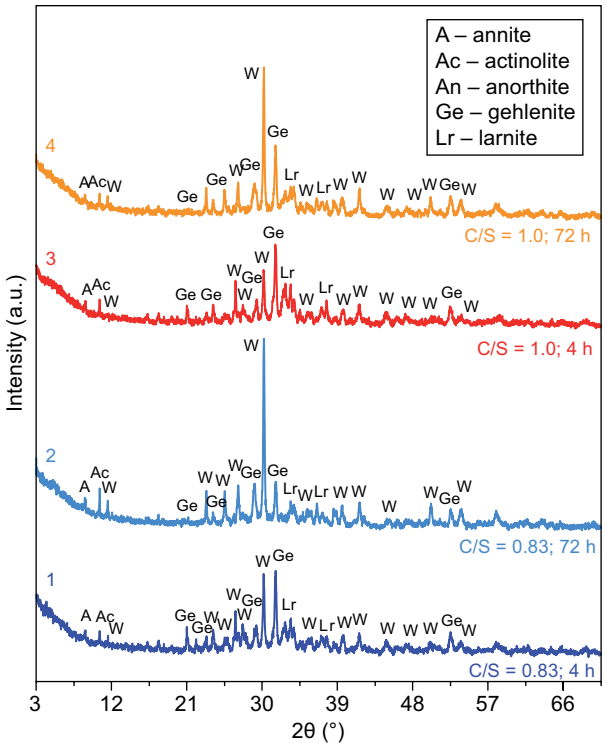

Figure 9. The XRD patterns of the synthesis products at 180 °C after calcination at 940 °C.

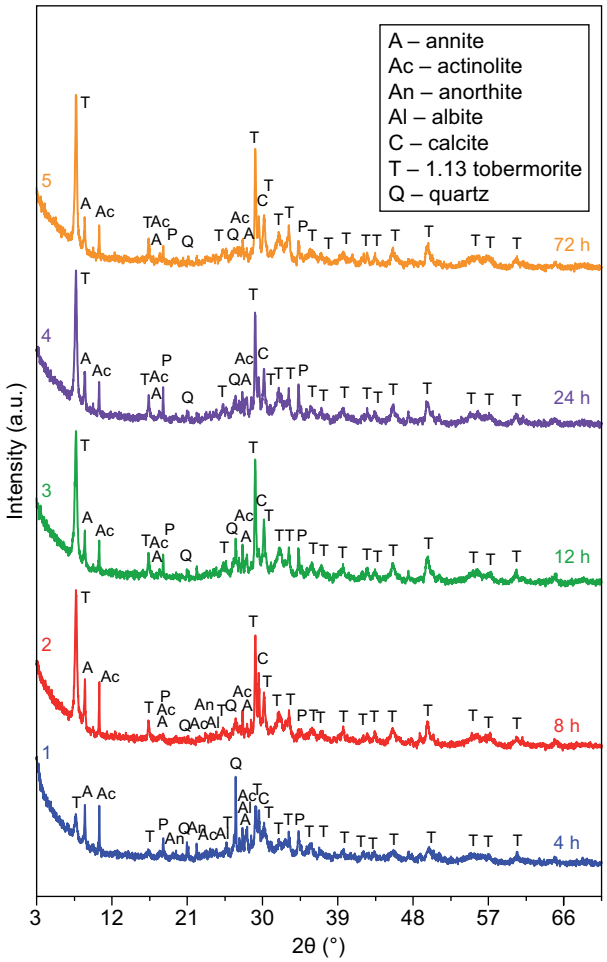

Figure 10. The XRD patterns of the synthesis products at 200 °C after 4 (1), 8 (2), 12 (3), 24 (4) and 72 h (5), when CaO/SiO_2 = 0.83.

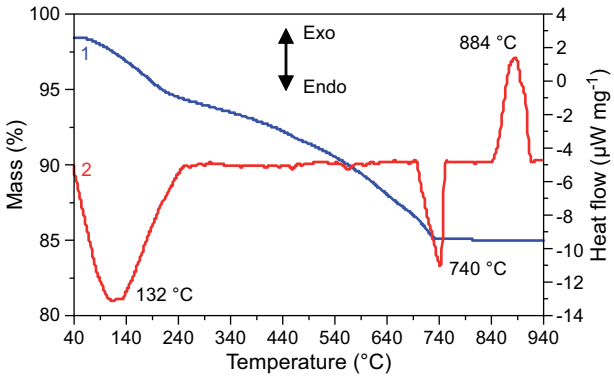

Figure 11. DSC and TG curves of the synthesis products at 200 °C after 4 h, when CaO/SiO_2 = 0.83.

higher than that obtained at 180 °C (Figure 3, curve 2). Thus, when the synthesis is carried out at 200 °C, 1.13 nm tobermorite becomes the dominant compound after 8 h and its peaks' intensity equals the product synthesised at 180 °C within 72 h. By prolonging the duration of the synthesis (Figure 10, curves 3−5), no significant changes occur, and the intensity of the tobermorite peaks remains almost unchanged. This means, the resulting 1.13 tobermorite is completely crystallised and becomes a dominant compound. It may be concluded that the 1.13 tobermorite of the highest crystallinity degree is formed during 8 h of synthesis, i.e., 9 times faster than in the case of the hydrothermal synthesis at 180 °C.

Furthermore, the peak intensity of the granite minerals such as annite (d = 1.01 nm) and actinolite (d = = 0.845 nm) is gradually, but constantly, decreasing with the prolonged hydrothermal synthesis duration up to 72 h.

For the mixture with a molar ratio CaO/SiO_2 = 0.83, it was found that 1.13 nm tobermorite is stable at 200 °C and does not recrystallise to other calcium silicate hydrates even within 72 h. In order to determinate the impact of the mixture's molar ratio on the stability of this compound, the mixture with a molar ratio of CaO/SiO_2 = 1.0 was examined at 200 °C as well. Already after 4 h of isothermal curing, 1.13 nm tobermorite becomes the dominant mineral (Figure 12, curve 1). Even after 72 h of hydrothermal curing, xonotlite is not detectable in the product (Figure 12, curve 2).

Moreover, the 1.13 nm tobermorite does not begin to recrystallise under these conditions into a thermodynamically stable calcium silicate hydrate (xonotlite). The composition of which is described by the molar ratio CaO/SiO_2 = 1.0, corresponds to the stoichiometric composition of the initial mixture. Presumably, this is due to the 15.4 % of Al_2O_3 contained in the granite sawing powder waste. There are a lot of data in the literature indicating that Al^{3+} ions isomorphically interrupt the 1.13 nm tobermorite crystal lattice, stabilise it, and prevent its recrystallisation into other compounds.

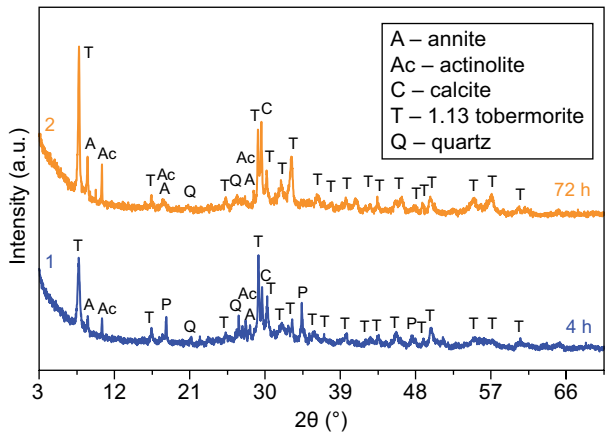

Figure 12. The XRD patterns of the synthesis products at 200 °C after 4 (1) and 72 h (2), when CaO/SiO_2 = 1.0.

CONCLUSIONS

- Granite sawing powder waste is a suitable material for fast 1.13 nm tobermorite synthesis. The amount of this compound in the products increases gradually, but constantly, by prolonging the isothermal curing duration at 180 °C to 72 h. By increasing the hydrothermal treatment temperature to 200 °C, a 1.13 tobermorite of a very high crystallinity degree forms during 8 h.
- At the beginning of the 1.13 nm tobermorite synthesis, semi-amorphous, without a clear crystal structure, calcium silicate hydrates form and consist of two phases: C–S–H(II) and C–S–H(I). When prolonging the hydrothermal curing duration, more and more SiO_2 reacts and calcium silicate hydrates with a stoichiometric composition close to the initial mixture's molar ratio (CaO/SiO_2 = 0.83 - 1.0) form.
- The formation of 1.13 nm tobermorite in the lime–granite sawing powder mixture goes much faster when the molar ratio CaO/SiO_2 is 0.83 than 1.0. This mineral is durable and does not transform into a thermodynamically stable calcium silicate hydrate, xonotlite, even at 200 °C with CaO/SiO_2 = 1.0, which corresponds to the stoichiometry of the latter compound.

Acknowledgements

This research was funded by a grant (No. S-MIP-17-92) from the Research Council of Lithuania.

REFERENCES

1. Hong S., Glasser F. (2004): Phase relations in the CaO–SiO_2–H_2O system to 200 C at saturated steam pressure. *Cement and Concrete Research,* 34, 1529-1534. doi: 10.1016/j.cemconres.2003.08.009
2. Baltakys K., Siauciunas R. (2007): The influence of γ-Al_2O_3 and Na_2O on the formation of calcium silicate hydrates in the CaO–quartz–H_2O system. *Materials Science-Poland,* 25, 185-198.
3. Paradiso P., R. Santos R., Horta R., Lopes J., Ferreira P., Colaço R. (2018): Formation of nanocrystalline tobermorite in calcium silicate binders with low C/S ratio. *Acta Materialia, 152*, 7-15. doi: 10.1016/j.actamat.2018.04.006
4. Viehland D., Yuan L. J., Xu Z., Cong X., Kirkpatrick R. J. (1997): Structural studies of jennite and 1.4 nm tobermorite: disordered layering along the [100] of jennite. *Journal of the American Ceramic Society. 80*, 3021-3028. doi: 10.1111/j.1151-2916.1997.tb03228.x
5. Mitsuda T., Taylor H. (1978): Normal and anomalous tobermorites. *Mineralogical Magazine, 42*, 229-235. doi: 10.1180/minmag.1978.042.322.09
6. Baltakys K., Iljina A., Bankauskaite, A. (2015): Thermal properties and application of silica gel waste contaminated with F^- ions for C–S–H synthesis. *Journal of Thermal Analysis and Calorimetry, 121*, 145-154. doi: 10.1007/s10973-015-4663-4

7. Bernstein S., Fehr K. (2012): The formation of 1.13 nm tobermorite under hydrothermal conditions: 1. The influence of quartz grain size within the system $CaO–SiO_2–D_2O$. *Progress in Crystal Growth and Characterization of Materials, 58,* 84-91. doi: 10.1016/j.pcrysgrow.2012.02.006
8. Smalakys G., Siauciunas R. (2018): The synthesis of 1.13 nm tobermorite from carbonated opoka. *Journal of Thermal Analysis and Calorimetry, 134*, 493-502. doi: 10.1007/s10973-018-7418-1
9. Hartmann A., Khakhutov M., Buhl J. (2014): Hydrothermal synthesis of C–S–H-phases (tobermorite) under influence of Ca-formate. *Materials Research Bulletin, 51,* 389-396. doi: 10.1016/j.materresbull.2013.12.030
10. Kikuma J., Tsunashima M., Ishikawa T., Matsuno S. Y., Ogawa A., Matsui K., Sato M. (2010): X-Ray Diffraction of Tobermorite Formation Process Under Autoclave Condition. Journal of the American Ceramic Society, *93*, 2667-2674. doi: 10.1111/j.1551-2916.2010.03815.x
11. Baltakys K., Siauciunas R. (2007): Gyrolite Formation in $CaO–SiO_2źnH_2O$ gamma $Al_2O_3–Na_2O–H_2O$ System under Hydrothermal Conditions. *Polish Journal of Chemistry, 81*, 103-114.
12. Aitken, A., Taylor H. (1960): Hydrothermal reactions in lime-quartz pastes. *Journal of Applied Chemistry, 10*, 7-15. doi: 10.1002/jctb.5010100104
13. McConnell J. D. (1954): The hydrated calcium silicates riversideite, tobermorite, and plombierite. *Mineralogical Magazine and Journal of the Mineralogical Society, 30*, 293-305. doi: 10.1180/minmag.1954.030.224.02
14. Eℓ-Hemaly S. A. S., Mitsuda T., Taylor, H. F. W. (1977): Synthesis of normal and anomalous tobermorites. *Cement and Concrete Research, 7*, 429-438. doi: 10.1016/0008-8846(77)90071-0
15. Galvánková L., Másilko J., Solný, T. Štěpánková E. (2016): Tobermorite synthesis under hydrothermal conditions. *Procedia Engineering, 151*, 100-107. doi: 10.1016/j.proeng.2016.07.394
16. Sarkar R., Das S. K., Mandal P. K., Maiti H. S. (2006): Phase and microstructure evolution during hydrothermal solidification of clay–quartz mixture with marble dust source of reactive lime. *Journal of the European Ceramic Society, 26*, 297-304. doi: 10.1016/j.jeurceramsoc.2004.11.006
17. Ríos C. A., Williams C. D. Fullen M. A. (2009): Hydrothermal synthesis of hydrogarnet and tobermorite at 175 °C from kaolinite and metakaolinite in the $CaO–Al_2O_3–SiO_2–H_2O$ system: A comparative study. *Applied Clay Science, 43*, 228-237. doi: 10.1016/j.clay.2008.09.014
18. Liu S., Han C., Liu J., Li, H. (2015): Hydrothermal decomposition of potassium feldspar under alkaline conditions. *Rsc. Advances, 5*, 93301-93309. doi: 10.1039/C5RA17212H
19. Youssef H., Ibrahim D., Komarneni S., Mackenzie K. (2010): Synthesis of 11 Å Al-substituted tobermorite from trachyte rock by hydrothermal treatment. *Ceramics International, 36*, 203-209. doi: 10.1016/j.ceramint.2009.07.004
20. Maeshima T., Noma H., Sakiyama M., Mitsuda T. (2003): Natural 1.1 and 1.4 nm tobermorites from Fuka, Okayama, Japan: Chemical analysis, cell dimensions, 29Si NMR and thermal behavior. *Cement and Concrete Research, 33*, 1515-1523. doi: 10.1016/S0008-8846(03)00099-1
21. Siauciunas R., Mikaliunaite J., Urbonas L., Baltakys K. (2014): Tribochemical and thermal activation of α-c2s hydrate as precursor for cementitious binders. *Journal of Thermal Analysis and Calorimetry, 118*, 817-823. doi: 10.1007/s10973-014-3921-1
22. Li H., Hui J., Wang C., Bao W., Sun Z. (2015): Removal of sodium (Na_2O) from alumina extracted coal fly ash by a mild hydrothermal process. *Hydrometallurgy, 153*, 1-5. doi: 10.1016/j.hydromet.2015.02.001
23. Jiménez I., Pérez G., Guerrero A., Ruiz B. (2017): Mineral phases synthesized by hydrothermal treatment from biomass ashes. *International Journal of Mineral Processing, 158*, 8-12. doi: 10.1016/j.minpro.2016.11.002
24. Ding J., Tang Z., Ma S., Wang Y., Zheng S., Zhang Y., Xie, Z. (2016): A novel process for synthesis of tobermorite fiber from high-alumina fly ash. *Cement and Concrete Composites,* 65, 11-18. doi: 10.1016/j.cemconcomp.2015.10.017
25. Tsutsumi T., Nishimoto S., Kameshima Y. Miyake M. (2014): Hydrothermal preparation of tobermorite from blast furnace slag for Cs and Sr2 sorption. *Journal of Hazardous Materials, 266*, 174-181. doi: 10.1016/j.jhazmat.2013.12.024
26. Wang S., Peng X., Tang L., Zeng L. Lan C. (2014): Influence of inorganic admixtures on the 11 Å-tobermorite formation prepared from steel slags: XRD and FTIR analysis. *Construction and Building Materials, 60*, 42-47. doi: 10.1016/j.conbuildmat.2014.03.002
27. Reinik J., Heinmaa I., Mikkola J., Kirso U. (2008): Synthesis and characterization of calcium–alumino-silicate hydrates from oil shale ash–Towards industrial applications. *Fuel, 87*, 1998-2003. doi: 10.1016/j.fuel.2007.11.008
28. Coleman N. J. (2005): Synthesis, structure and ion exchange properties of 11 Å tobermorites from newsprint recycling residue. *Materials Research Bulletin, 40*, 2000-2013. doi: 10.1016/j.materresbull.2005.05.006
29. Houston J.R., Maxwell R. S., Carroll S. A. (2009): Transformation of meta-stable calcium silicate hydrates to tobermorite: reaction kinetics and molecular structure from XRD and NMR spectroscopy. *Geochemical Transactions, 10(1)*, 1. doi: 10.1186/1467-4866-10-1
30. Mostafa N., Shaltout A., Omar H., Abo-El-Enein S. (2009): Hydrothermal synthesis and characterization of aluminium and sulfate substituted 1.1 nm tobermorites. *Journal of Alloys and Compounds, 467*, 332-337. doi: 10.1016/j.jallcom.2007.11.130
31. Shaw S., Clark S., Henderson C. (2000): Hydrothermal formation of the calcium silicate hydrates, tobermorite ($Ca_5Si_6O_{16}(OH)_2·4H_2O$) and xonotlite ($Ca_6Si_6O_{17}(OH)_2$): an in situ synchrotron study. *Chemical Geology, 167*, 129-140. doi: 10.1016/S0009-2541(99)00205-3
32. Xi Y., Glasse, L. D. (1984): Hydrothermal study in the system Na_2O-CaO-SiO_2-H_2O at 300 °C. *Cement and Concrete Research, 14*, 741-748. doi: 10.1016/0008-8846(84)90037-1
33. Nelson E. B., Kalousek G. L. (1977): Effects of Na_2O on calcium silicate hydrates at elevated temperatures. *Cement and Concrete Research, 7*, 687-694. doi: 10.1016/0008-8846(77)90052-7
34. NocuÒ-Wczelik W. (1999): Effect of Na and Al on the phase composition and morphology of autoclaved calcium silicate hydrates. *Cement and Concrete Research, 29*, 1759-1767. doi: 10.1016/S0008-8846(99)00166-0
35. Suzuki S., Sinn E. (1993): 1.4 nm Tobermorite-like calcium silicate hydrate prepared at room temperature from $Si(OH)_4$ and $CaCl_2$ solutions. *Journal of Materials Science Letters, 12*, 542-544. doi: 10.1007/BF00278317

36. Chen M., Lu L., Wang S., Zhao P., Zhang W., Zhang S. (2017): Investigation on the formation of tobermorite in calcium silicate board and its influence factors under autoclaved curing. *Construction and Building Materials,* 143, 280-288. doi: 10.1016/j.conbuildmat.2017.03.143
37. Meller N., Hall C., Phipps J. S. (2005): A new phase diagram for the $CaO–Al_2O_3–SiO_2–H_2O$ hydroceramic system at 200 °C. *Materials Research Bulletin, 40(5)*, 751-723. doi: 10.1016/j.materresbull.2005.03.001
38. Taylor H. (1959): The transformation of tobermorite into xonotlite. *Mineralogical Magazine and Journal of the Mineralogical Society, 32*, 110-116. doi: 10.1180/minmag.1959.32.245.03
39. Zou J., Guo C., Jiang Y., Wei C., Li, F. (2016): Structure, morphology and mechanism research on synthesizing xonotlite fiber from acid-extracting residues of coal fly ash and carbide slag. *Materials Chemistry and Physics, 172*, 121-128. doi: 10.1016/j.matchemphys.2016.01.050
40. Guo X., Meng F., Shi H. (2017): Microstructure and characterization of hydrothermal synthesis of Al-substituted tobermorite. *Construction and Building Materials, 133*, 253-260. doi: 10.1016/j.conbuildmat.2016.12.059
41. Grangeon S., Claret F., Lerouge C., Warmont F., Sato T., Anraku, S., Numako C., Linard Y., Lanson B. (2013): On the nature of structural disorder in calcium silicate hydrates with a calcium/silicon ratio similar to tobermorite. *Cement and Concrete Research, 52*, 31-37. doi: 10.1016/j.cemconres.2013.05.007
42. Dhanapandiana S., Shanthib, M. (2009): Utilization of marble and granite wastes in brick products. *Journal of Industrial Pollution Control, 25*, 145-150.
43. Segadães A., Carvalho M., Acchar W. (2005): Using marble and granite rejects to enhance the processing of clay products. *Applied Clay Science, 30*, 42-52. doi: 10.1016/j.clay.2005.03.004
44. Siauciunas R., Rupsyt E., Kitrys S., Galeckas V. (2004): Influence of tobermorite texture and specific surface area on CO_2 chemisorption. *Colloids and Surfaces A: Physicochemical and Engineering Aspects, 244(1-3),* 197-204. doi: 10.1016/j.colsurfa.2004.06.004
45. Biagioni C., Bonaccorsi E., Lezzerini M., Merlino S. (2016): Thermal behaviour of Al-rich tobermorite. *European Journal of Mineralogy*, *28*(1), 23-32. doi: 10.1127/ejm/2015/ 0027-2499
46. Jackson M. D., Moon J., Gotti E., Taylor R., Chae S. R., Kunz M., et al. (2013): Material and elastic properties of Al-tobermorite in ancient Roman seawater concrete. *Journal of the American Ceramic Society*, *96*(8), 2598-2606. doi: 10.1111/jace.12407
47. Cong X., Kirkpatrick R. J. (1996): 29Si MAS NMR study of the structure of calcium silicate hydrate. *Advanced Cement Based Materials*, *3*(3-4), 144-156. doi: 10.1016/S1065-7355(96)90046-2
48. Nonat A. (2004): The structure and stoichiometry of C–S–H. *Cement and Concrete Research*, *34*(9), 1521-1528. doi: 10.1016/j.cemconres.2004.04.035